CORROSION SCIENCE AND TECHNOLOGY, Vol.20, No.2(2021), pp.62~68
[Research Article]
pISSN 1598-6462 / eISSN 2288-6524
DOI: https://doi.org/10.14773/cst.2021.20.2.62

An Experimental Investigation of the Application of Artificial Neural Network Techniques to Predict the Cyclic Polarization Curves of AL-6XN Alloy with Sensitization

Kwang-Hu Jung[1] and Seong-Jong Kim[2,†]

[1]*Mokpo branch, Korea institute of maritime and fisheries technology, Mokpo, Jeonnam,58625, Korea*
[2]*Division of Marine Engineering, Mokpo Maritime University, Mokpo, Jeonnam, 58628, Korea*
(Received April 02, 2021; Revised April 07, 2021; Accepted April 08, 2021)

Artificial neural network techniques show an excellent ability to predict the data (output) for various complex characteristics (input). It is primarily specialized to solve nonlinear relationship problems. This study is an experimental investigation that applies artificial neural network techniques and an experimental design to predict the cyclic polarization curves of the super-austenitic stainless steel AL-6XN alloy with sensitization. A cyclic polarization test was conducted in a 3.5% NaCl solution based on an experimental design matrix with various factors (degree of sensitization, temperature, pH) and their levels, and a total of 36 cyclic polarization data were acquired. The 36 cyclic polarization patterns were used as training data for the artificial neural network model. As a result, the supervised learning algorithms with back-propagation showed high learning and prediction performances. The model showed an excellent training performance (R^2=0.998) and a considerable prediction performance (R^2=0.812) for the conditions that were not included in the training data.

Keywords: *Artificial neural network, AL-6XN, Cyclic polarization curve, Sensitization, Environmental variable*

1. Introduction

The super austenitic stainless steel (SASS) is applied to various industrial fields owing to excellent corrosion resistance, mechanical properties and weldability in a severely corrosive environment. However, it can be vulnerable to corrosion such as pitting, crevice corrosion, intergranular corrosion (IGC), and stress corrosion cracking.

The localized corrosion is sensitive to environmental parameters such as chloride ion, temperature and pH [1,2]. Furthermore, when exposed to the temperature range of 500-850 ºC, SASS is sensitized due to the secondary phase precipitation at grain boundaries [3,4].

Predicting the corrosion properties is the essential step for controlling corrosion in the use environment. However, it is difficult to analyze and predict the factors because each factor is involved in the growth through complex interactions among various environmental parameters, including degree of sensitization (DOS). Moreover, the cyclic potentiodynamic polarization (CPDP) test of the electrochemical method for assessing the localized corrosion properties of stainless steel is nonlinear and represents highly complex relationships between variables and reaction values. The machine learning (ML) technique can be applied to the data analysis of such unspecified and complex relationships.

Currently, ML is drawing attention in various industries and scientific studies, and its performance is being proven in a variety of applications. Among the ML techniques, an artificial neural network (ANN) is a statistical learning algorithm inspired by the biological neural networks (especially the brain of animals' central nervous system) in cognitive science. ANN shows excellent performance in the prediction (output) for various complex characteristic data (input). It is primarily specialized in solving nonlinear relationship problems.

Since the factors of the localized property of stainless steel show complex interactions, it is highly likely that the factors and response characteristic values would not show a linear relationship. Therefore, it is expected that using the high performance of ANN in nonlinear problem solving can be used to achieve high performance in predicting the polarization curve of stainless steel. Moreover, this performance has been proven in preliminary studies [5,6].

This study aims to generate an ANN prediction model

†Corresponding author: ksj@mmu.ac.kr
Kwang-Hu Jung: Professor, Seong-Jong Kim: Professor

with the environmental parameters (temperature, pH) for the pitting corrosion behavior of AL-6XN with DOS. The prediction model was generated using the ANN technique of supervised learning. The experiment was conducted in a 3.5% NaCl solution according to the experimental matrix with various levels of each factor for training data. A total of 36 CPDP curves were obtained and used as training data. Finally, the prediction model was validated under random test conditions not included in the training data.

2. Experimental Methods

2.1 Material and tensile tests

The chemical composition of the SASS AL-6XN is 0.02 wt% C, 0.27 wt% Si, 0.56 wt% Mn, 0.03 wt% P, 0.01 wt% S, 20.2 wt% Cr, 6.83 wt% Mo, 24.8 wt%. Ni, 0.61 wt% Cu, and Fe for the rest. For sensitization, heat-treatment was performed for up to 12 hours in an electric heat furnace elevated to 800 ºC, and the completed specimens were quenched in fresh water at room temperature. Each plate was cut into small specimens with 10 mm × 10 mm × 5 mm, and the surface was polished to remove scales formed by the heat-treatment.

2.2 Assessment of DOS

The DOS was assessed using the double loop electrochemical reactivation (DL-EPR) test with a three-electrode corrosion cell composed of a working, counter, and reference electrodes, and VSP potentiostat (Biologic). For the counter and reference electrodes, a platinum mesh with 20 mm × 20 mm and Ag/AgCl (sat. by KCl) were used. The surface of the heat-treatment specimen of the working electrode was polished up to #2000 of SiC paper, and finally polished using 1 μm alumina powder. Then ultrasonic cleaning was performed to remove foreign substances and oil in ethanol and distilled water. The working electrode exposed a reaction area of 1 cm^2 using a self-made holder. The test medium was a 2M H_2SO_4 + 0.01M KSCN + 2M NaCl solution at 30 ºC. The open circuit potential(OCP) was measured after immersion in the test solution for 30 min. Polarization was performed from OCP to +300 mV. Thereafter, it was performed in the reverse direction until the OCP. The scan rate was the same at 1.667 mV/s. Each experiment was performed three times to obtain reproducibility of the electrochemical measurements. The DOS from the DL-EPR curve was calculated using equation (1):

$$DOS=(I_a/I_r) \times 100 \quad (1)$$

where I_a is the current density peak of the activation section, and I_r is the current density peak of the reactivation section. This study did not present a polarization curve for the DL-EPR test.

2.3 CPDP test

The DOS, temperature, and pH were designed to levels 4, 3, and 3. The details are presented in Table 1. The CPDP test used a three-electrode corrosion cell under the 3.5 % NaCl solution at 25 ºC. The OCP was measured after immersing the specimen in each test solution for 30 min. Polarization was performed from the OCP of -0.25 V and once the current density reached 5 mA/cm^2, it was performed in a reverse direction to the OCP. The scan rate in the polarization is the same at 0.5 mV/s. Each experimental condition was presented to the matrix in Table 2, and a total of 36 cyclic polarization curve data were obtained.

2.4 Artificial neural network

The CPDP curve represents the current density (log i) values according to the change of potential (E). In short, the prediction target is to predict the current density at the potential change in a given environmental variable. As shown in Fig. 1, the artificial neural network model is the back-propagation algorithm of multiple layer perceptron (MLP), which consists of an input layer with four nodes, a double-hidden layer, and output layer. The hyperbolic tangent (*tanh*) was applied to the activation function for each

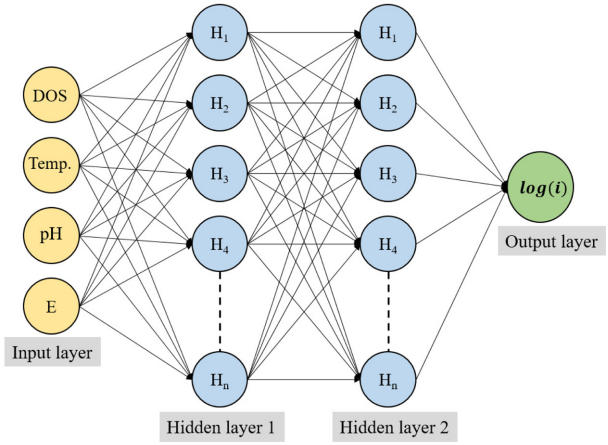

Fig. 1. Schematic diagram for ANN architecture used for modeling polarization curves

hidden layer. The ratios of training, validation, and test data used in the neural network are 80%, 10%, and 10%, and the data were selected randomly in model training. The Python 3.7 and Tensorflow 2.0 libraries were used for the design and operation of the neural network. The mean squared error (MSE) of equation (2) was used as the cost function.

$$\frac{1}{n}\sum_{1}^{n}\left(X(t)-X'(t)\right)^2 \quad (2)$$

where n is the number of output for the training set, $X(t)$ is the actual value, and $X'(t)$ is the prediction value. For optimization of the cost function, the Adam (Adaptive Moment Estimation) algorithm was used.

3. Results and Discussion

3.1 Microstructure

Fig. 2 shows a scanning electron microscope(SEM) image for microstructure of AL-6XN with heat-treatment time. The nano-sized σ phase precipitated at the grain boundary grows continuously by consuming the surrounding Cr and Mo. As a result, Cr and Mo depleted-zone are formed around it, and the metal becomes highly sensitive to IGC. In Fig. 2a, the base metal was consists of γ phase austenite structure. On the other hand, a needle-shaped secondary phase was precipitated at the grain boundary, and the size and number tended to increase with time, as Fig. 2b,c. Fig. 2d shows SEM and energy-dispersive X-ray spectroscopy (EDX) analysis results for secondary phase powder that was electronically extracted from the specimen heat-treated at 800 °C. Mo and Cr increased compared to the new austenite base, but Ni and Fe decreased. In particular, Mo was abundant at 23.5 wt% compared to the austenite base (6.83 wt%).

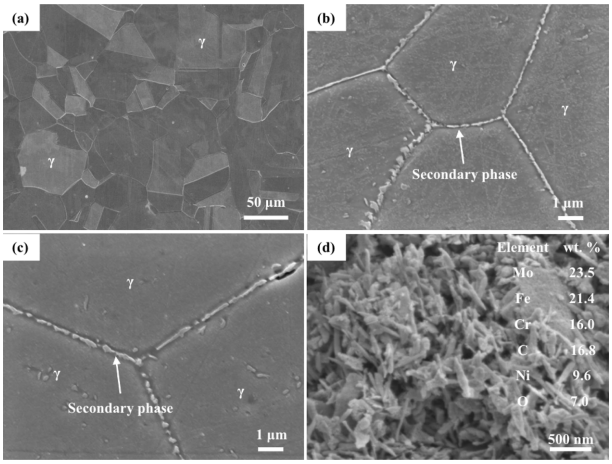

Fig. 2. The microstructure of AL-6XN alloy heat-treated at 800 °C: (a) as-received, (b) 3 hours, (c) 12 hours, (d) electronically extracted secondary phase from Fig. 2(c)

3.2 Quantification of DOS

The temperature and pH are quantified input variables provided for the ANN model. By contrast, DOS is an experimental value obtained from an engineering experiment, and as such, deviations may occur in the result values obtained from repetitive experiments under the same conditions. For efficient training of the ANN model, quantified DOS values are required. To quantify the DOS, it was fitted by the logistic function of equation 3, and the results are shown in Fig. 3.

$$y = A_2 + \frac{(A_1 - A_2)}{(1 + (x/x_o)^p)} \quad (3)$$

where A_1 is the initial value, A_2 is the final value, X_o is the mean value, and p is the constant for power function. The Levenberg-Marquardt algorithm was used for the optimization of the regression line [7]. The logistic function was found to be the most suitable function that can express the incubation, increment, and stagnation periods that appear in the metal's sensitization phenomenon. The coefficient of determination (R^2) for the regression curve is 0.9878. To validate the regression curve, a validation experiment was conducted for a specimen degraded for 4 hours, which is not included in the training data. The experimental and predicted values respectively were 42.08 and 39.98, and satisfied the

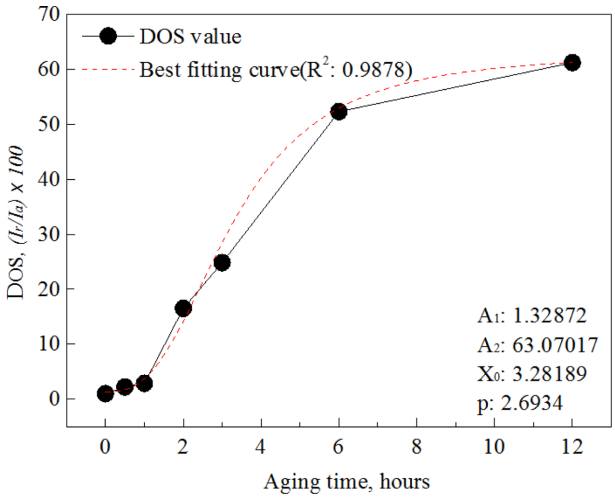

Fig. 3. Fitted curve for DOS value

Table 1. Designed factors and their levels

Factors	Unit	Level			
		1	2	3	4
Heat-treatment time (DOS): A	hours	0(1)	1(3)	3(28)	6(53)
Temperature: B	°C	25	50	75	-
pH: C		2	4	6	-

95% confidence interval. The sensitization degree calculated through the fitting curve is shown in Table 1.

3.3 ANN model

Determining the appropriate numbers of hidden layers and neurons is the most important element for creating an ANN model with excellent performance. No methodology for optimizing the numbers of hidden layers and neurons has been developed until now. The ANN model must be optimized through repetitive trials and errors [8]. Basically, the back-propagated ANN model is composed of an input layer, an output layer, and one or more hidden layers connected to the neuron processor. It has been proven through various studies that a single hidden layer is sufficient for learning a continuous function [9]. However, to learn a pattern with discontinuities such as the CPDP curve requires two or more hidden layers [10]. The number of neurons of the hidden layer can vary by the data pattern and format, and the number of input layers. Lachtermacher and Fuller [11] proposed a methodology for determining the number of neurons of the hidden layer as the following equation (4):

$$0.11P \le NHN(I+1) \le 0.3P \tag{4}$$

where I is the number of input neurons, and P is the number of training patterns. The neuron number based on Equation (4) ranges from 24 to 72. In this study, the ANN performance was assessed in various structures by expanding the range of the neurons number from 10 to 100. Table 3 shows the performance of the ANN model with the number of neurons of the double hidden layer to which the S-shaped hyperbolic activation function was applied. The performance was assessed using the MSE of equation (2) and the R^2. As shown in Table 3, the MSE and the R^2 tended to improve with the increasing number of neurons. With 70 neurons, the MSE and the R^2 improved to 0.0024 and 0.999, respectively. However, with more than 70 neurons, no performance improvement was observed. A wider and deeper structure of the ANN shows a higher performance, but the computation time and cost increase. Furthermore, the prediction performance may be degraded due

Table 2. Experiment design matrix for CPDP tests in 3.5% NaCl solution

Input parameter							
Row	DOS	Temp., °C	pH	Row	DOS	Temp., °C	pH
1	0	25	2	17	3	75	4
2	0	25	4	18	3	75	6
3	0	25	6	19	22	25	2
4	0	50	2	20	22	25	4
5	0	50	4	21	22	25	6
6	0	50	6	22	22	50	2
7	0	75	2	23	22	50	4
8	0	75	4	24	22	50	6
9	0	75	6	25	22	75	2
10	3	25	2	26	22	75	4
11	3	25	4	27	22	75	6
12	3	25	6	28	53	25	2
13	3	50	2	29	53	25	4
14	3	50	4	30	53	25	6
15	3	50	6	31	53	50	2
16	3	75	2	32	53	50	4

to over-fitting for the training data. Therefore, in this study, we used 4-70-70-1 as the optimal structure.

3.4 Validation of ANN model

Fig. 4 compares the actual curve and the prediction curve for some test conditions in the ANN learning data. The curve patterns matched well, and the OCP and pitting potentials were also highly similar. This result proved that the ANN model can predict the CPDP curve with each environmental parameter.

Table 3. Comparison of performance of ANN structure with hidden neurons number ranging from 10 to 100

Architecture	Training		Validation	
	MSE	R^2	MSE	R^2
4-10-10-1	0.0827	0.939	0.0937	0.937
4-20-20-1	0.017	0.989	0.013	0.989
4-30-30-1	0.0097	0.992	0.0105	0.992
4-40-40-1	0.0037	0.994	0.0077	0.993
4-50-50-1	0.0029	0.998	0.0021	0.998
4-60-60-1	0.0034	0.996	0.0043	0.996
4-70-70-1	0.0024	0.999	0.0055	0.999
4-80-80-1	0.0064	0.993	0.0061	0.992
4-90-90-1	0.0036	0.999	0.0052	0.999
4-100-100-1	0.0023	0.996	0.0041	0.996

Fig. 5 shows the correlations between the actual values and the predicted values of the ANN model. Most data points are close to the best regression line (Y=T) with the R^2 of 1, and showed a very high correlation. The R^2 for the training, validation and test sets were very high at 0.99 at the minimum.

Fig. 6 compares the actual curves and prediction curves for new conditions not included in the ANN model. The patterns of the curves did not perfectly match. However, the overall pattern and electrochemical characteristic values were highly similar, and the R^2 for the curves in Fig. 6a-d is 0.812. Although this is lower than the R^2 of 0.998 for the training data, it is believed that an acceptable level of prediction performance was obtained considering the unique corrosion characteristics of stainless steel and the flexibility, complexity, and reproducibility of engineering experiments.

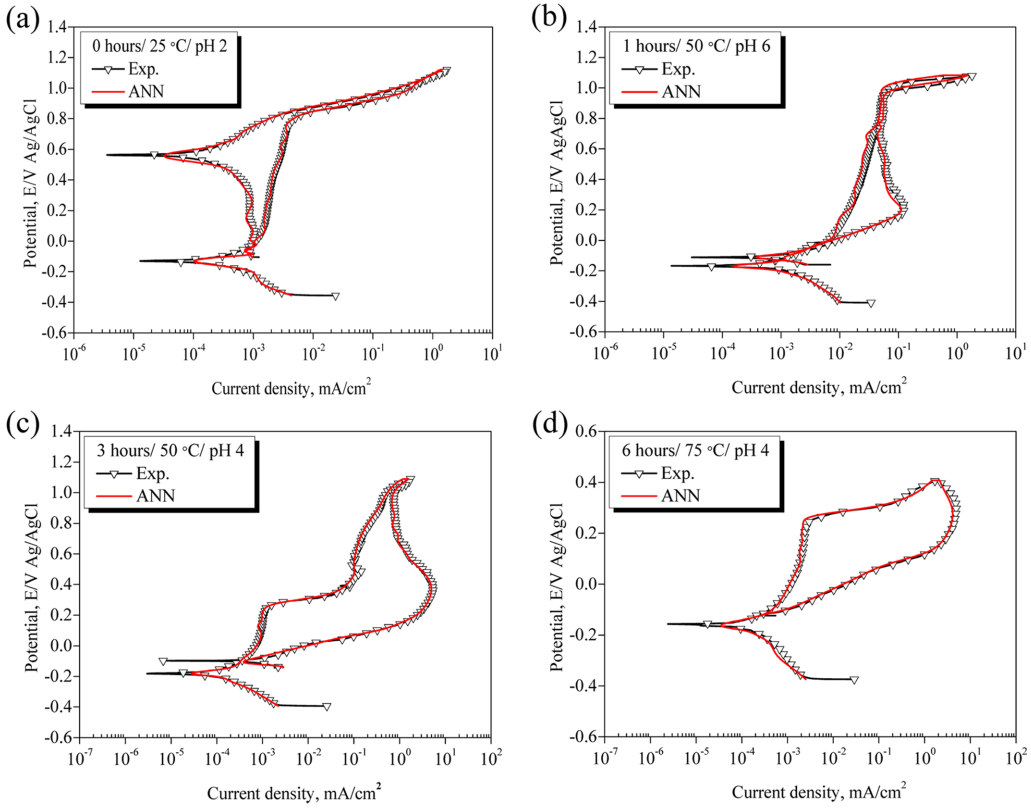

Fig. 4. Experimental and ANN predicted polarization curves for some train data. These conditions included in Table 2

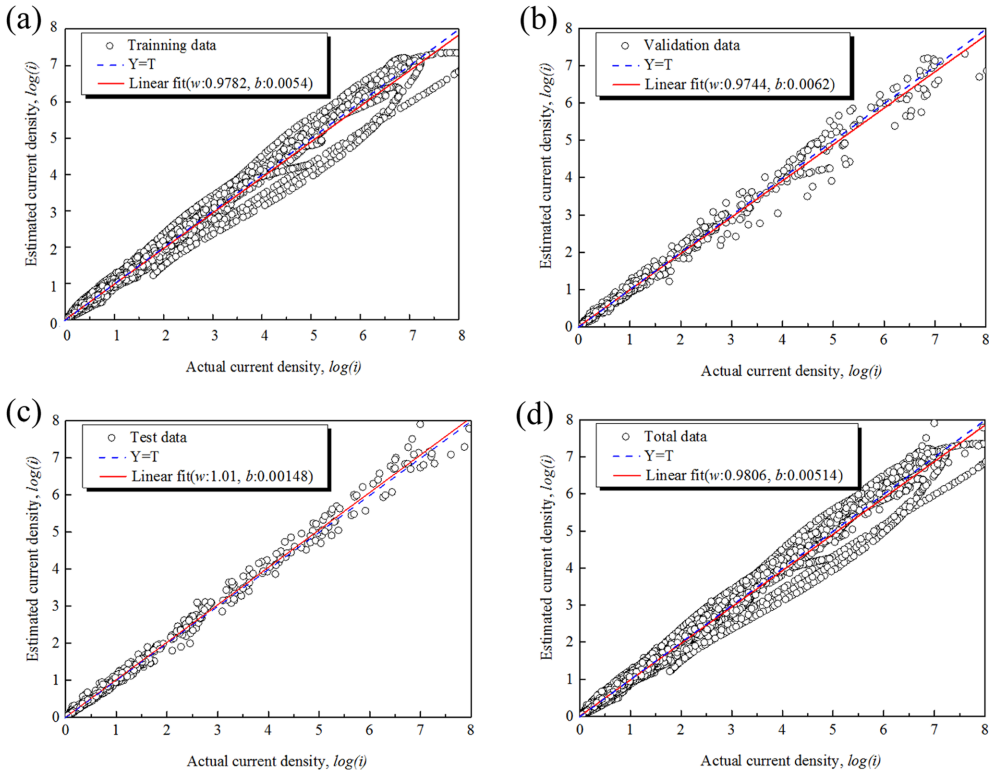

Fig. 5. Diagram of actual values vs. predicted values for log(i): (a) training data set: 34,184 plots, (b) validation data set: 3,799 plots, (c) test data set: 4,279 plots, (d) total data set: 42,781 plots

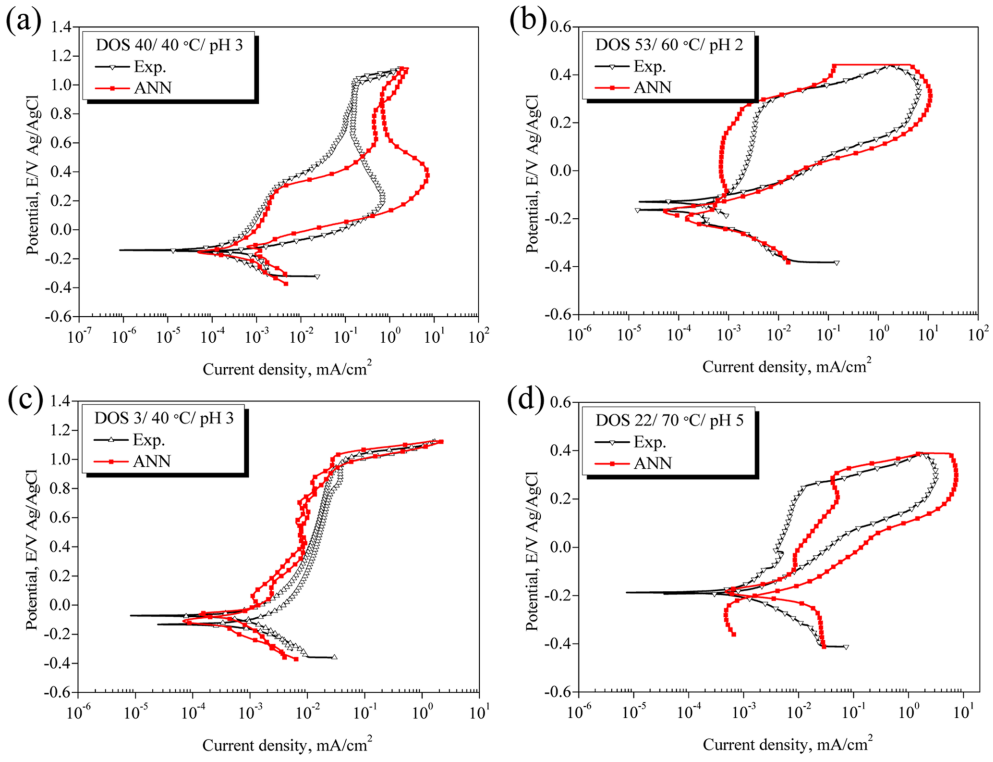

Fig. 6. Experimental and ANN predicted polarization curves. These conditions not included in Table 2

4. Conclusions

This study applied the ANN technique of supervised learning with temperature and pH variations of sensitized AL-6XN in a 3.5% NaCl solution. The supervised learning ANN of back-propagation showed high learning and prediction performances. It showed a very high learning performance (R^2=0.998) for CPDP curves in forward and reverse directions, and acceptable performance (R^2=0.812) was obtained for validation data not included in the training data as well. The ANN model can be highly effective for prediction for corrosion characteristics of complex relationships with input parameters. The prediction performance of the ANN model could be improved further by training with additional data that includes more factors and levels.

Acknowledgments

This research was a part of the project titled 'Demonstration of aftertreatment systems of Ship's air pollutant (NOx/SOx/PM) and establishment of their certification system', funded by the Ministry of Oceans and Fisheries, Korea.

References

1. Z. Cui, S. Chen, Y. Dou, S. Han, L. Wang, C. Man, X. Wang, S. Chen, Y. F. Chen, and X. Li, Passivation behavior and surface chemistry of 2507 super duplex stainless steel in artificial seawater: Influence of dissolved oxygen and pH, *Corrosion Science*, **150**, 218 (2019). Doi: https://doi.org/10.1016/j.corsci.2019.02.002
2. R. T. Loto, Effect of elevated temperature variations on the corrosion resistance of S31603 and SS2562 austenitic stainless steels in chloride-sulphate environments, *Journal of Materials Research and Technology*, **8**, 5415 (2019). Doi: https://doi.org/10.1016/j.jmrt.2019.09.008
3. H. M. Jang, D. J. Kim, and H. P. Kim, Sensitivity to Intergranular Corrosion According to Heat Treatment of 304L Stainless Steel, *Corrosion Science and Technology,* **19**, 37 (2020). Doi: https://doi.org/10.14773/cst.2020.19.1.37
4. Z. G. Song and E. X. Pu, Precipitated phases of superaustenitic stainless steel 654SMO, *Journal of Iron and Steel Research International*, **24**, 743 (2017). Doi: https://doi.org/10.1016/S1006-706X(17)30112-7
5. Q. Hu, Y. Liu, T. Zhang, S. Geng, and F. Wang, Modeling the corrosion behavior of Ni-Cr-Mo-V high strength steel in the simulated deep sea environments using design of experiment and artificial neural network, *Journal of Materials Science & Technology*, **35**, 168 (2019). Doi: https://doi.org/10.1016/j.jmst.2018.06.017
6. C. L. C. Roxas and B. A. Lejano, An artificial neural network model for the corrosion current density of steel in mortar mixed with seawater, *International Journal of GEOMATE*, **16**, 79 (2019). Doi: https://doi.org/10.21660/2019.56.4585
7. M. T. Hagan and M. B. Menhaj, Training feedforward networks with the Marquardt algorithm, *IEEE Transactions on Neural Networks*, **5**, 989 (1994). Doi: https://doi.org/10.1109/72.329697
8. C. I. Rocabruno-Valdés, J. G. González-Rodriguez, Y. Díaz-Blanco, A. U. Juantorena, J. A. Muñoz-Ledo, Y. El-Hamzaoui, and J. A. Hernández, Corrosion rate prediction for metals in biodiesel using artificial neural networks, *Renewable Energy*, **140**, 592 (2019). Doi: https://doi.org/10.1016/j.renene.2019.03.065
9. G. Jiang, J. Keller, P. L. Bond, and Z. Yuan, Predicting concrete corrosion of sewers using artificial neural network, *Water Research*, **92**, 52 (2016). Doi: https://doi.org/10.1016/j.watres.2016.01.029
10. J. Sun, L. Fang, and J. Han, Optimization of concrete hollow brick using hybrid genetic algorithm combining with artificial neural networks, *International Journal of Heat and Mass Transfer,* **53**, 5509 (2010). Doi: https://doi.org/10.1016/j.ijheatmasstransfer.2010.07.006
11. G. Lachtermacher and J. D. Fuller, Back propagation in time series forecasting, *Journal of Forecasting,* **14**, 381 (1995). Doi: https://doi.org/10.1002/for.3980140405